



## CRITICAL INCIDENT ANGLE FOR THE MINIMUM COST DESIGN OF LOW, MID AND HIGH-RISE STEEL AND REINFORCED CONCRETE-COMPOSITE BUILDINGS

Ch.Ch. Mitropoulou<sup>1</sup> and N.D. Lagaros<sup>1,2\*, †</sup>

<sup>1</sup>*Institute of Structural Analysis & Antiseismic Research, Department of Structural Engineering, School of Civil Engineering, National Technical University of Athens, 9, Heroon Polytechniou Str., Zografou Campus, GR-15780 Athens, Greece*

<sup>2</sup>*iOPTI, Consulting and Design Optimization Group, École Polytechnique, X-Up, Avenue Coriolis, 91128 Palaiseau Cedex, Paris, France*

### ABSTRACT

One of the main tasks of engineers is to design structural systems light and economic as possible, yet resistant enough to withstand all possible loads arising during their service life and to absorb the induced seismic energy in a controlled and predictable fashion. The traditional trial-and-error design approach is not capable to determine an economical design satisfying also the code requirements. Structural design optimization, on the other hand, provides a numerical procedure that can replace the traditional design approach with an automated one. The objective of this work is to propose a performance-based seismic design procedure, formulated as a structural design optimization problem, for designing steel and steel-concrete composite buildings subject to interstorey drift limitations. In particular a straightforward design procedure is proposed where the influence on both record and incident angle is considered. For this purpose six test examples are considered, in particular three steel and three steel-concrete composite buildings are optimally designed for minimum initial cost.

**Keywords:** performance-based design; fibre modelling; steel and steel-reinforced concrete composite buildings; incident angle; metaheuristic optimization.

Received: 20 August 2015; Accepted: 3 October 2015

---

\*Corresponding author: School of Civil Engineering, National Technical University of Athens, 9, Heroon Polytechniou Str., Zografou Campus, GR-15780 Athens, Greece

†E-mail address: nlagaros@central.ntua.gr (N.D. Lagaros)

## 1. INTRODUCTION

The modern approach to structural design for the case of seismic or wind loading is based on the principal that a structure should meet performance objectives for a number of hazard levels. This approach constitutes the performance-based design (PBD) concept, which has been introduced in order to increase the safety against natural hazards. According to PBD the structures should be able to resist all loading conditions arising during their service life in a quantifiable manner and to present levels of desired possible damage. The current state of practice in performance-based engineering for the case of earthquake loading can be found in US guidelines such as ASCE-41 [1], FEMA-445 [2] and ATC-58 [3]. Towards this goal, these guidelines suggest higher-order analysis procedures for the design and assessment in seismic prone areas.

Among others [4,5], incremental dynamic analysis (IDA) [6] is considered as an analysis procedure for obtaining good estimates of the structural performance in the case of earthquake hazard and it is considered as an appropriate method to be incorporated into the optimization procedure. In view of the complexity and the computational effort required by the 3D models, that are employed to represent real buildings, simplified 2D structural simulations are used during the design procedure, therefore it is not possible to employ a 2D simulation since the bidirectional orthogonal shaking effects should be taken into account. In studies by the authors [7,8] multicomponent incremental dynamic analysis (MIDA) has been proposed. Multicomponent incremental dynamic analysis (MIDA) is performed in a similar way that the 2D implementation of IDA does, i.e. a suit of records is selected and for each record an MIDA representative curve is derived. The 50% fractile MIDA curve is then calculated using the representative curves of all the records. Selecting the IDA representative curve in its 2D implementation is, in most cases, a straightforward procedure. On the other hand in its 3D implementation is not an easy task, since the incident angle selected for applying the two components of the records might influence considerably the product of MIDA [7,8].

A highly efficient design framework can be offered by structural optimisation taking advantage of the benefits offered by nonlinear, static or dynamic analysis methods. PBD formulated as a structural optimisation problem is a topic of growing interest and has been the subject of extensive research over the last years. Advancements in structural optimisation have made possible the move from traditional trial-and-error design procedures towards fully automated approaches based on a structural optimisation search-engine. This is mostly attributed to the rapid development of metaheuristic optimization methods, which are capable of handling complicated design optimization problems.

In recent years, steel-reinforced concrete composite buildings have been experiencing increased use worldwide. This is because reinforced concrete (RC) is not expensive and RC members are stiff; on the other hand steel members are strong, lightweight and easy to assemble. In composite columns two systems are commonly used: (i) steel reinforced concrete members, where a steel section is encased in concrete and (ii) concrete filled tubes. In many cases, the choice of either of the two systems is based on their excellent resistance to seismic loading. The objective of this work is the formulation of a performance-based optimum design framework for designing steel and steel-RC composite moment resisting building structures subject to interstorey drift limitations with reference to their initial cost

where the influence of the seismic incident angle is examined by means of MIDA. In particular a straightforward design procedure is proposed where the influence on both record and incident angle is considered. For this purpose low, mid and high-rise steel and steel-RC composite 3D buildings are considered. More specifically six test examples are considered, in particular three steel and three steel-concrete composite buildings are optimally designed with minimum initial cost.

## 2. SURVEY ON PERFORMANCE-BASED DESIGN OPTIMIZATION

A number of studies have been published in the past where the concept of performance-based design optimization was studied. Among others, Fuyama *et al.* [9] presented a computer-based design methodology for the control of interstorey drift caused by equivalent static earthquake loads in tall moment resisting steel frame structures. Beck *et al.* [10] presented a general framework for multi-criteria optimal design, which is well suited for performance-based design of structural systems operating in an uncertain dynamic environment. Ganzerli *et al.* [11] proposed a performance-based optimization procedure of reinforced concrete (RC) frames using a mathematical optimizer. Esteva *et al.* [12] presented a life-cycle formulation for the determination of optimum values of the mechanical properties of a structural system exposed to seismic risk. The resulting values were used for the establishment of performance-acceptance criteria for seismic design. Khajehpour and Grierson [13] investigated the trade-off between life-cycle profitability and load-path safety for a high-rise office-building project, while they proposed alternative building layouts with increased safety using a multi-criterion genetic algorithm (GA). Li and Cheng [14] introduced a damage reduction based technique in the framework of structural optimization and showed that the proposed design concept leads to designs with better seismic performance in terms of both life-cycle cost and maximum interstorey drift criteria. Chan and Zou [15] presented an effective optimization technique for the elastic and inelastic drift performance design of reinforced concrete buildings under response spectrum loading and pushover loading. Liu *et al.* [16] proposed a GA-based multi-objective structural optimization procedure for steel frames considering four objective functions; weight, maximum interstorey drift for two performance levels, and design complexity criteria. Chan and Wang [17] developed an optimality criteria based algorithm for solving the minimum weight design problem subject to multiple drift constraints and member sizing requirements. Fragiadakis *et al.* [18] proposed a performance-based optimization procedure for steel moment-resisting frames in the probabilistic framework of FEMA-350 [19]. Fragiadakis *et al.* [20] proposed a new methodology for the performance-based optimum design of steel structures subjected to seismic loading considering inelastic behaviour, while the importance of considering life-cycle cost as an additional objective to the initial structural cost objective function in the context of multi-objective optimization was also investigated. Foley *et al.* [21] presented an overview of a state-of-the-art model-code performance-based design methodology and implemented this design procedure into multiple-objective optimization problems for single and multi-storey structural steel frameworks with fully and partially restrained connections. Lagaros and Papadrakakis [22] evaluated the European seismic design code when used for the design of 3D reinforced concrete buildings, versus a PBD

procedure, in the framework of a multi-objective optimization concept. Rojas *et al.* [23] used GA to solve this complex optimization problem where confidence levels were incorporated into the fitness function along with initial construction cost in a series of optimal design scenarios. A fully automated design methodology based on nonlinear response history analysis was proposed by Fragiadakis and Papadrakakis [24] for the optimum seismic design of reinforced concrete structures. Mitropoulou *et al.* [25] assessed the European seismic design codes and in particular of EC2 and EC8 with respect to the recommended behaviour factor  $q$  into an optimization framework. Lagaros *et al.* [26] proposed a PBD methodology for the design of reinforced concrete buildings, taking into account the influence of infill walls, while two variants of the PBD framework are examined relying either on the non-linear static or on the non-linear dynamic analysis procedure. Kaveh *et al.* [27] presented a performance-based optimal seismic design of frame structures using the ant colony optimization method. The current state-of-practice static pushover methods as suggested in the provisions of European and American regulations are implemented in a comparative study by Lagaros and Fragiadakis [28], in a performance-based design optimization framework. Esteva *et al.* [29] presented an overview of life-cycle optimisation in the establishment of reliability and performance-based seismic design requirements for multi-storey systems. Al-Ansari and Senouci [30] presented a drift design structural model for the design optimization of high-rise buildings in seismic zones. Fragiadakis and Lagaros [31] presented a general PBD optimization framework for steel structures; while in Mitropoulou *et al.* [32] presented a multiobjective life-cycle optimisation problem examining the parameters that affect the LCCA procedure. Lagaros and Magoula [33] employed life-cycle cost analysis (LCCA) for assessing the optimum designs obtained for steel and steel-concrete composite design practices. Kaveh *et al.* [34] dealt with design optimization of real size 3D steel structures under seismic loading based on response spectral and equivalent static analyses, investigated also the effect of lateral seismic loading distribution on the achieved optimum designs.

### 3. CRITICAL ORIENTATION OF THE SEISMIC INCIDENCE

A structure subjected to the simultaneous action of two orthogonal horizontal ground accelerations along the directions  $O_w$  and  $O_p$  is illustrated in Fig. 1. The orthogonal system  $O_{xyz}$  defines the reference axes of the structure (structural axes). The angle defined with a counter clockwise rotation of the structural axis  $O_x$  to coincide with the ground motion axis  $O_w$  is called as incident angle of the record.

According to Penzien and Watabe [35] the orthogonal directions of a ground motion can be considered uncorrelated in the principal directions of the structure. This finding was the basis for many researchers in order to define the orientation that yields the maximum response when the response spectrum dynamic analysis was applied. In the work by Wilson *et al.* [36] it was proposed an alternative code approved method that results in structural designs having equal resistance to seismic motions from all directions. Lopez and Torres [37] proposed a simple method, which can be employed by the seismic codes to determine the critical angle of seismic incidence and the corresponding peak response of structures subjected to two horizontal components applied along any arbitrary directions and to the

vertical component of earthquake ground motion. The CQC3 response spectrum rule for combining the contributions from three orthogonal components of ground motion to the maximum value of a response quantity is presented in the work by Menun and Der Kiureghian [38]. In two works by Lopez *et al.* [39,40] it is proposed an explicit formula, convenient for code applications, in order to calculate the critical value of the structural response to the two principal horizontal components acting along any incident angle with respect to the structural axes, and the vertical component of ground motion. In two works by Menun and Der Kiureghian [41,42] a response spectrum based procedure for predicting the envelope that bounds two or more responses in a linear structure is developed. In the work by Anastassiadis *et al.* [43] a seismic design procedure for structures is proposed based on the model of Penzien and Watabe [35].

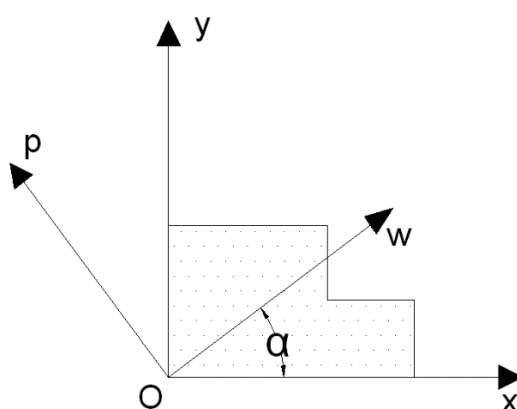


Figure 1. Definition of the incident angle  $\alpha$

To the author's knowledge there are only few studies reported in the literature where the case of the critical incident angle is examined when time history analysis is employed. In these studies it was found that it is not an easy task to define the critical angle, while it is record dependent when nonlinear structural behaviour is encountered. In the work by MacRae and Mattheis [44] it is shown the ability of the 30% SRSS rule and the sum of absolute values methods to assess building drifts for bidirectional shaking effects, while it is also shown that the response is dependent on the reference axes chosen. MacRae and Tagawa [45] have found that design level shaking caused the structure to exceed story yield drifts in both directions simultaneously and significant column yielding occurred above the base. Shaking a structure in the direction orthogonal to the main shaking direction increased drifts in the main shaking direction, indicating that 2D analyses would not estimate the 3D response well. Ghersi and Rossi [46] examined the influence of bi-directional seismic excitations on the inelastic behaviour of in-plan irregular systems having one symmetry axis where it was found that in most cases the adoption of Eurocode 8 provisions to combine the effects of the two seismic components allows the limitation of the orthogonal elements ductility demand. In the work by Athanatopoulou [47] analytical formulae were developed for determining the critical incident angle and the corresponding maximum value of a response quantity of structures subjected to three seismic correlated components when linear behaviour is considered. The analyses results have shown that, for the earthquake records used, the critical value of a response quantity can be up to 80% larger than the usual

response produced when the seismic components are applied along the structural axes. Rigato and Medina [48] studied a number of symmetrical and asymmetrical structures having fundamental periods ranging from 0.2 to 2.0 seconds where it was examined the influence that the incident angle of the ground motion has on several engineering demand parameters. Lagaros [8] assessed four 3D reinforced concrete buildings with reference to life cycle cost calculated based on MIDA and the significance of considering randomness on both record and incident angle is demonstrated.

#### 4. PERFORMANCE-BASED SEISMIC DESIGN

The majority of the seismic design codes belong to the category of the prescriptive design codes that take into consideration site selection and development of the conceptual, preliminary and final design stages. According to a prescriptive design code the strength of the structure is evaluated at one limit state, between life-safety and near collapse, using a response spectrum-based loading corresponding to one or two design earthquakes (e.g. Eurocode 8, 2004). In addition, the serviceability limit state is usually checked in order to ensure that the structure will not deflect or vibrate excessively. On the other hand, performance-based design implies the design, evaluation, construction and maintenance of engineering facilities in order to meet the objectives set by the society and owners/users of a facility [49]. In the case of seismic loading, the aim is to build structures having a predictable and reliable performance, or in other words, to be able to resist earthquakes with quantifiable confidence. Therefore, the modern conceptual approach of seismic structural design is that the structures should meet performance-based objectives for a number of different hazard levels ranging from earthquakes with a small intensity and with a small return period, to more destructive events with large return periods. The current state of practice in performance-based earthquake engineering is defined by US guidelines [1-3]. These guidelines do not differ conceptually and introduce procedures that can be considered as the first significant diversification from prescriptive building design codes. For the PBD procedure, prior to any structural analysis, the column to beam strength ratio is calculated and is examined whether the sections chosen are of class 1, as Eurocode 3 [50] suggests. Class 1 cross-sections are those, which can form a plastic hinge with the rotation capacity required from plastic analysis without reduction of the resistance. The column to beam strength ratio is calculated as:

$$\frac{\sum M_{pl,column}}{\sum M_{pl,beam}} \geq 1.20 \quad (1)$$

where  $\sum M_{pl,column}$  and  $\sum M_{pl,beam}$  is the sum of the design values of plastic moment resistances of the structural members at each joint.

The PBD procedure consists of the following steps: (i) All Eurocode checks must be satisfied for the gravity loads; (ii) if the checks of Step (i) are satisfied then NSP is performed in order to explicitly calculate the demand for the defined intensity levels. The structural capacity is associated to the maximum interstorey drift values  $\theta$ , and the

acceptance criteria of Step (ii) are confirmed if satisfied or not in order to accept or revise the design. The main part in a performance-based seismic design procedure is the definition of the performance objectives. A performance objective is defined as a given level of performance for a specific hazard level. In order to assess the structural performance in terms of strength and deformation capacity globally as well as at the element level a nonlinear analysis procedure is required. In this work the PBD framework is based on the nonlinear dynamic procedure (NDP) and in particular MIDA. Three performance levels are considered and 20 ground motion records are used for each hazard level. For each hazard level the median response out of the 20 records is used. The characteristics of the records are provided in Table 1.

Table 1: Characteristics of the group of 20 records

Record/Station	R <sup>1</sup> (km)	EpiD <sup>2</sup> (km)	Recording Angle log/tran (°)	Duration (sec)	PGA <sub>log</sub> (g)	PGA <sub>tran</sub> (g)	Campbell's GEOCODE <sup>3</sup>	Fault rupture <sup>4</sup>
Superstition Hills 1987 (B) (M=6.7)								
El Centro Imp. Co Cent Wildlife Liquefaction Array	18.5	35.83	000/090	40.00	0.36	0.26	A	SS
Imperial Valley 1979 [23:16], (M=6.5)								
Chihuahua	8.4	18.88	012/282	40.00	0.27	0.25	A	SS
Compuertas	15.3	24.43	015/285	36.00	0.19	0.15	A	SS
Plaster City	31.1	54.26	045/135	18.75	0.042	0.057	A	SS
El Centro Array #12	18.85	31.99	140/230	39.00	0.143	0.116	A	SS
El Centro Array #13	22.83	35.95	140/230	39.50	0.117	0.139	A	SS
San Fernando 1971 (M=6.6)								
LA, Hollywood Stor. Lot Northridge 1994 (M=6.7)	25.9	39.49	090/180	28.00	0.21	0.17	A	RN
<b>Leona Valley #2</b>	<b>37.2</b>	<b>51.88</b>	<b>000/090</b>	<b>32.00</b>	<b>0.09</b>	<b>0.06</b>	<b>A</b>	<b>RN</b>
LA, Baldwin Hills	29.9	28.20	090/360	40.00	0.24	0.17	C	RN
<b>Lake Hughes #1</b>	<b>89.67</b>	<b>93.22</b>	<b>000/090</b>	<b>32.00</b>	<b>0.087</b>	<b>0.077</b>	<b>A</b>	<b>RN</b>
LA, Hollywood Stor FF	114.62	118.2	090/360	40.00	0.231	0.358	A	RN
LA, Centinela St.	31.53	32.72	155/245	30.00	0.465	0.322	A	RN
Loma Prieta 1989 (M=6.9)								
Hollister Diff Array	24.8	45.10	165/255	39.64	0.27	0.28	A	RO
<b>WAHO</b>	<b>17.5</b>	<b>12.56</b>	<b>000/090</b>	<b>24.96</b>	<b>0.37</b>	<b>0.64</b>	<b>C</b>	<b>RO</b>
Halls Valley	30.5	36.31	000/090	39.95	0.13	0.10	B	RO
Agnews State Hospital	24.6	40.12	000/090	40.00	0.17	0.16	A	RO
Anderson Dam (Downstream)	4.4	16.67	270/360	39.61	0.244	0.240	B	RO
Coyote Lake Dam (Downstream)	20.8	30.89	195/285	39.95	0.160	0.179	B	RO
Hollister - South & Pine	27.93	48.24	000/090	60.00	0.371	0.177	A	RO

<sup>1</sup>Campbell's R Distance<sup>2</sup>Distance from the recording site to epicentre<sup>3</sup>Campbell's site classification: A (Firm Soil), B (Very Firm Soil), C (Soft Rock), D (Firm Rock), E (Shallow Soils)<sup>4</sup>Fault rupture mechanism: SS (Strike Slip), N (Normal), RN (Reverse-Normal), RO (Reverse-Oblique), NO (Normal- Oblique)

## 5. MULTICOMPONENT INCREMENTAL DYNAMIC ANALYSIS USED FOR DESIGN OF STRUCTURES

In the seismic assessment and design procedures of structures a wide range of seismic records and more than one performance level should be considered in order to take into account the uncertainties that the seismic hazard introduces into a performance-based seismic assessment procedure. The methods integrated into the performance-based assessment procedures are classified as single and multiple hazard level methods. Multiple-stripe dynamic analysis (MSDA) and incremental dynamic analysis (IDA) or MIDA are the most applicable methods [7]. The main objective of these procedures is to define a relation between the seismic intensity level and the corresponding maximum response quantity of the structural system. The intensity level and the structural response are described through an intensity measures (IMs) and an engineering demand parameters (EDPs), respectively. EDP in some cases it refers also as damage index (DI). MSDA, IDA or MIDA are implemented through the following steps: (i) Define the nonlinear finite element model required for performing nonlinear dynamic analyses; (ii) select a suit of natural records or artificial accelerograms; (iii) select a proper intensity measure and an engineering demand parameter; (iv) employ an appropriate algorithm for selecting the record scaling factor in order to obtain the IM-EDP curve.

According to the MIDA framework a set of natural records, each one represented by its longitudinal and transverse components, are applied to the structure in order to account for the randomness on the seismic excitation. The difference of the MIDA framework from the original one component IDA, proposed by Vamvatsikos and Cornell [6], stems from the fact that for each record a number of MIDA representative curves can be defined depending on the incident angle selected, while in most cases of the one component variant of IDA only one IDA representative curve is obtained. MIDA is based on the idea of considering variable incident angle for each record, through this implementation randomness both on the seismic excitation and the incident angle are taken into account. In MIDA the relation of IM-EDP is defined similarly to the one component version of the IDA, i.e. both horizontal components of each record are scaled to a number of intensity levels to encompass the full range of structural behaviour from elastic to yielding that continues to spread, finally leading to global instability.

## 6. LOWER BOUND STRUCTURAL DESIGN

The ultimate objective of this study is to compare lower-bound designs, or in other words comparing the designs that satisfy design requirements in the most cost-effective way, i.e. those with minimum cross section dimensions, member and reinforcement steel quantities. For this reason, a structural optimization problem is formulated and the designs obtained are then assessed. The formulation of a structural optimization problem is defined as follows



$$\begin{aligned}
 & \min_{\mathbf{s} \in F} C_{IN}(t, \mathbf{s}) \\
 & \text{subject to } g_j^{SERV}(\mathbf{s}) \leq 0 \quad j=1, \dots, m \\
 & \quad \quad \quad g_j^{PBD}(\mathbf{s}) \leq 0 \quad j=1, \dots, k
 \end{aligned} \tag{2}$$

where  $\mathbf{s}$  represents the design vector with the cross-section dimensions of all columns and beams,  $F$  is the feasible region where all the serviceability and performance-based constraint functions ( $g^{SERV}$  and  $g^{PB}$ ) are satisfied, while the objective function considered is the initial cost  $C_{IN}$  of the design, which is related to material cost, which includes structural steel, concrete, steel reinforcement, construction labour costs and the cost of the non-structural elements. Additionally, the cost of the contents is included. The performance-based constraints considered are related to the maximum interstorey drift limits  $\theta$ . This is a commonly used measure of both structural and non-structural damage because of its close relationship to plastic rotation demands on individual beam-column connection assemblies. In this study three performance objectives are considered corresponding to hazard levels of 50, 10 and 2 percent probabilities of exceedance in 50 years. The detailed description of the exact steps followed for the seismic design of the buildings can be found in the work by Lagaros and Papadrakakis [22], while a flowchart of these steps is presented in Fig. 2, where a nonlinear static analysis method is nested in the iterative optimum design algorithm.

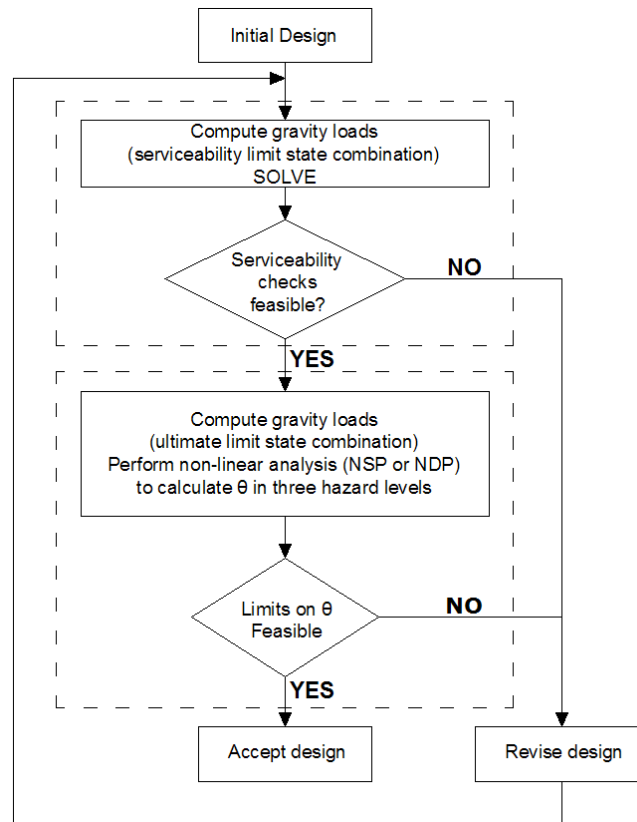


Figure 2. Flowchart of the proposed performance-based design procedure [22]

For the solution of the optimization problem the differential evolution method (DE), is employed. DE represents a direct search method which utilizes a population of  $NP$  parameter vectors  $s_{i,g}$  ( $i=1,\dots, NP$ ) for each generation  $g$ . DE generates new vectors by adding the weighted difference vector between two population members to a third member. If the resulting vector corresponds to a better objective function value than a population member, the newly generated vector replaces this member. The comparison is performed between the newly generated vector and all the members of the population excluding the three ones used for its generation. Furthermore, the best parameter vector  $s_{best,g}$  is evaluated in every generation in order to keep track of the progress achieved during the optimization process. Several variants of DE have been proposed so far, but the two most widely used are the following.

According to the variant implemented in this study, a donor vector  $v_{i,g+1}$  is generated first according to:

$$v_{i,g+1} = s_{i,g} + F \cdot (s_{r_2,g} - s_{r_3,g}) \quad (3)$$

Before the computation of the  $i^{\text{th}}$  parameter vector  $s_{i,g+1}$ . This step is equivalent to the mutation operator step of genetic algorithms or evolution strategies. The integers  $r_1, r_2$  and  $r_3$  are chosen randomly from the interval  $[1, NP]$  while  $i \neq r_1, r_2$  and  $r_3$ .  $F$  is a real constant value, called mutation factor, which controls the amplification of the differential variation  $(s_{r_2,g} - s_{r_3,g})$  and is defined in the range  $[0,2]$ . In the next step the crossover operator is applied by generating the trial vector  $u_{i,g+1} = [u_{1,i,g+1}, u_{2,i,g+1}, \dots, u_{D,i,g+1}]^T$  which is defined from the elements of the vector  $s_{i,g}$  and the elements of the donor vector  $v_{i,g+1}$  whose elements enter the trial vector with probability  $CR$  as follows:

$$u_{j,i,g+1} = \begin{cases} v_{j,i,g+1} & \text{if } \text{rand}_{j,i} \leq CR \text{ or } j = I_{rand} \\ s_{j,i,g} & \text{if } \text{rand}_{j,i} > CR \text{ or } j \neq I_{rand} \end{cases} \quad (4)$$

$$i = 1, 2, \dots, NP \text{ and } j = 1, 2, \dots, n$$

where  $\text{rand}_{j,i} \sim U[0,1]$ ,  $I_{rand}$  is a random integer from  $[1, 2, \dots, n]$  that ensures that  $v_{i,g+1} \neq s_{i,g}$ . The last step of the generation procedure is the implementation of the selection operator where the vector  $s_{i,g}$  is compared to the trial vector  $u_{i,g+1}$ :

$$s_{i,g+1} = \begin{cases} u_{i,g+1} & \text{if } f(u_{i,g+1}) \leq f(s_{i,g}) \\ s_{i,g} & \text{otherwise} \end{cases} \quad (5)$$

$$i = 1, 2, \dots, NP$$

## 7. MODELLING AND FINITE ELEMENT ANALYSIS

Nonlinear static or dynamic analysis needs a detailed simulation of the structure in the regions where inelastic deformations are expected to develop. Either the plastic-hinge or the

fibre approach can be adopted for this cause. Given that the plastic hinge approach has limitations in terms of accuracy fibre beam-column elements are preferable. According to the fibre approach, every beam-column element has a number of integration sections, each divided into fibres. Each fibre in the section can be assigned concrete, structural steel, or reinforcing bar material properties (see Fig. 3 for the case of a composite column). The sections are located either at the centre of the element or at its Gaussian integration points. The main advantage of the fibre approach is that every fibre has a simple uniaxial material model allowing an easy and efficient implementation of the inelastic behaviour. This approach is considered to be suitable for inelastic beam-column elements under dynamic loading and provides a reliable solution compared to other formulations. However, it results to higher computational demands in terms of memory storage and CPU time. When a displacement-based formulation is adopted the discretization should be adaptive with a dense mesh at the joints and a single elastic element for the remaining part of the member. On the other hand, force-based fibre elements allow modelling a member with a single beam-column element. All the frames are assumed to have rigid connections and fixed supports. In the numerical test examples section that follows, all analyses have been performed using the OpenSEES [51] platform and each member is modelled with force-based beam-column elements. A bilinear material model with pure kinematic hardening is adopted for the steel fibres, while geometric nonlinearity is explicitly taken into consideration. For the simulation of the concrete fibres the modified Kent-Park [52] model is employed while the bracing members are modelled using an inelastic element with pinned ends [53].

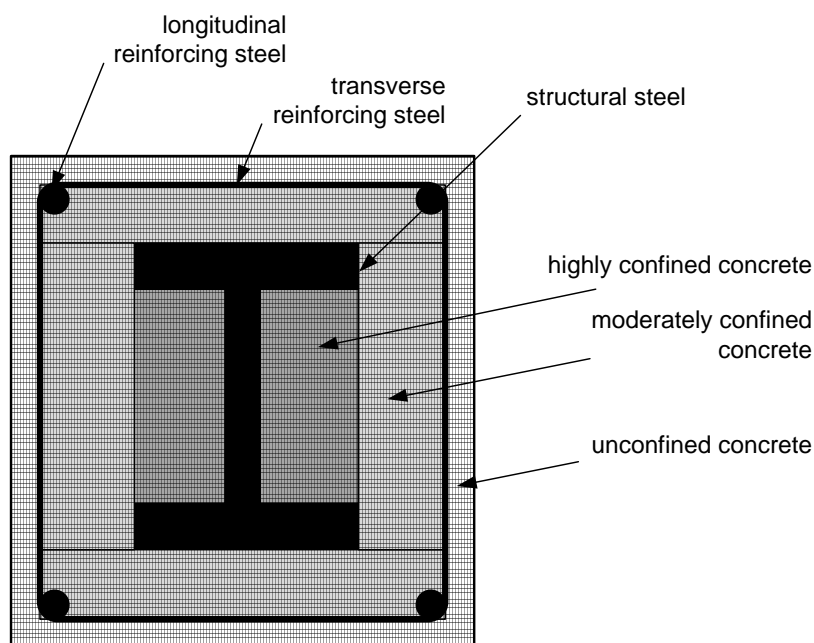


Figure 3. Fibre discretization of a composite section

## 8. NUMERICAL EXAMPLES

In this work, three steel and three steel-RC composite 3D moment resisting framed buildings have been considered in order to study the problem of performance-based design optimization. The first group of buildings corresponds to steel buildings with two, four and eight storeys; while the second one corresponds to steel-RC composite buildings also with two, four and eight-storeys. Fig. 4 depicts the plan view of the steel and steel-RC composite buildings along with the front view for the case of the eight-storey steel building with bracings. Steel of class with characteristic yield stress of 235 MPa and modulus of elasticity equal to 210 GPa has been considered while the concrete of the composite sections was of class with characteristic cylindrical strength of 20 MPa and modulus of elasticity equal to 30 GPa (corresponding to the moderately confined concrete of the composite section). Compared to the moderately confined concrete the cylindrical strength of the unconfined concrete is reduced by 20% while that of the highly confined one is increased by 10%. The slab thickness is equal to 12 cm, while in addition to the self-weight of the beams and the slabs, a distributed permanent load of 2 kN/m<sup>2</sup> due to floor finishing partitions and an imposed load of 1.5 kN/m<sup>2</sup>, are used.

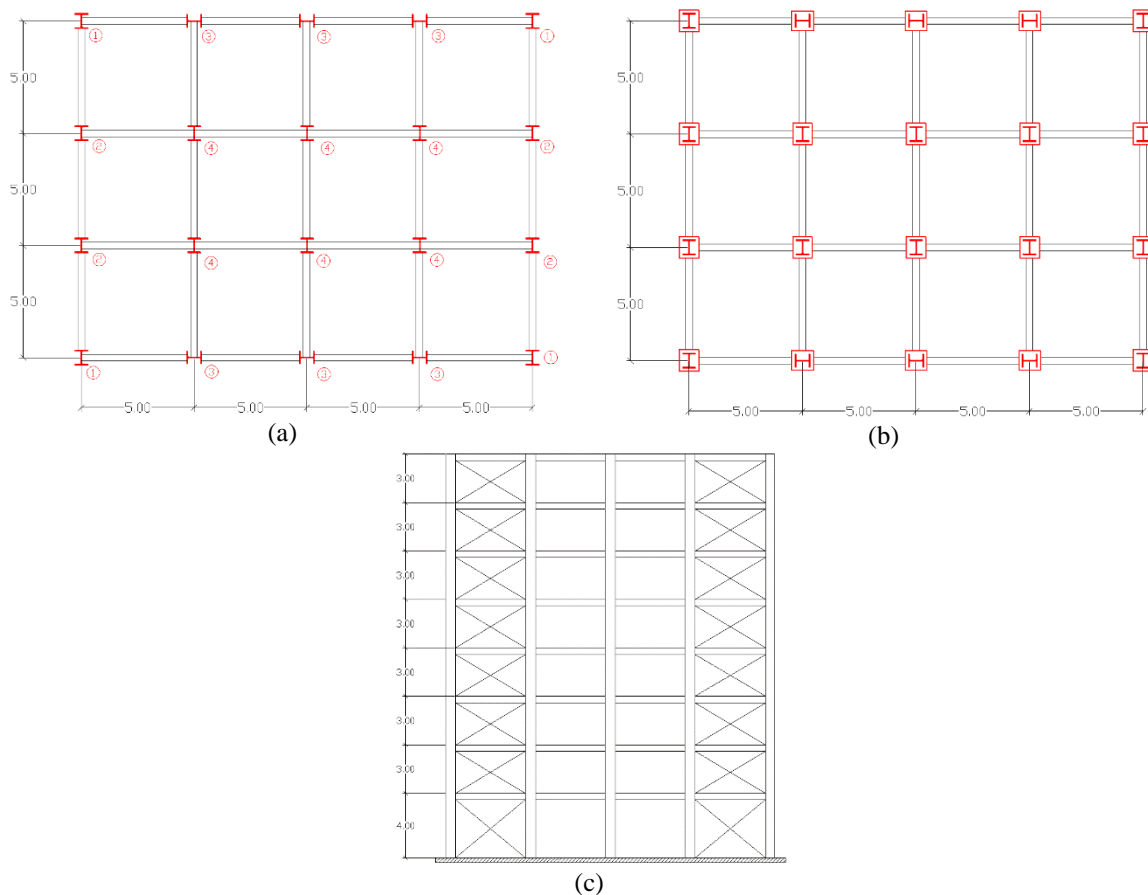


Figure 4. Test examples - (a) steel building plan view, (b) steel-RC composite building plan view and (c) eight-storey steel building front view

Two parts compose the numerical investigation. In the first part, in order to examine the influence of the incident angle on the seismic response of the structure, three records have been selected at random and are applied to steel test examples. The three records considered are the one recorded during the 1989 Loma Prieta earthquake (WAHO), and two recorded during the 1994 Northridge earthquake (Leona Valley #2 and Lake Huger #1). The three records are marked with bold letters in Table 1 and have been applied considering a varying incident angle in the range of 0 to 360 degrees with a step of 5 degrees. In order to examine the influence of the incident angle on the maximum interstorey drift to different intensity levels, the three records have been scaled with respect to the 5% damped spectral acceleration at the structure's first mode period to 0.05g, 0.15g, 0.30g and 0.50g, and the maximum interstorey drift has been recorded for all the incident angles and the intensity levels considered.

### 8.1 Parametric study

The relation of the maximum interstorey drift values with reference to the incident angle and the intensity level for three records is presented in Figs. 5 to 10 for the six test examples, respectively. As it can be seen from these figures the seismic response for all test examples when the incident angle varies in the range of 0 and 180 degrees almost coincides with the seismic response corresponding to incident angle varying in the range of 185 to 360 degrees. This is because the relative ratio of the two horizontal components of the records is close to one, thus the two components are scaled to almost the same intensity level, i.e. the same value of  $SA(T_1, 5\%)$ . A second remark from Figs. 5 to 10, is that the seismic response varies significantly with respect to the incident angle. For instance for the eight storey steel test example the maximum interstorey drift for the case of Loma Prieta (WAHO record) varies from 0.15% to 0.42% for the 0.05g intensity level (see Fig. 7a) while for the 0.50g intensity level the maximum interstorey drift for the same record varies from 1.32% to 4.52% (see Fig. 7d). Another significant observation from these figures is that the maximum seismic response is encountered for different incident angles when a different record is considered. Worth mentioning that for the 0.30g intensity level the maximum seismic response for example the four storey steel test example is encountered in the incident angle range of 10 degrees for the Loma Prieta (WAHO record). For the Leona Valley #2 record, however, in the same incident angle range the minimum seismic response is encountered (see Fig. 6c). Similar observations can be noticed for all test examples.

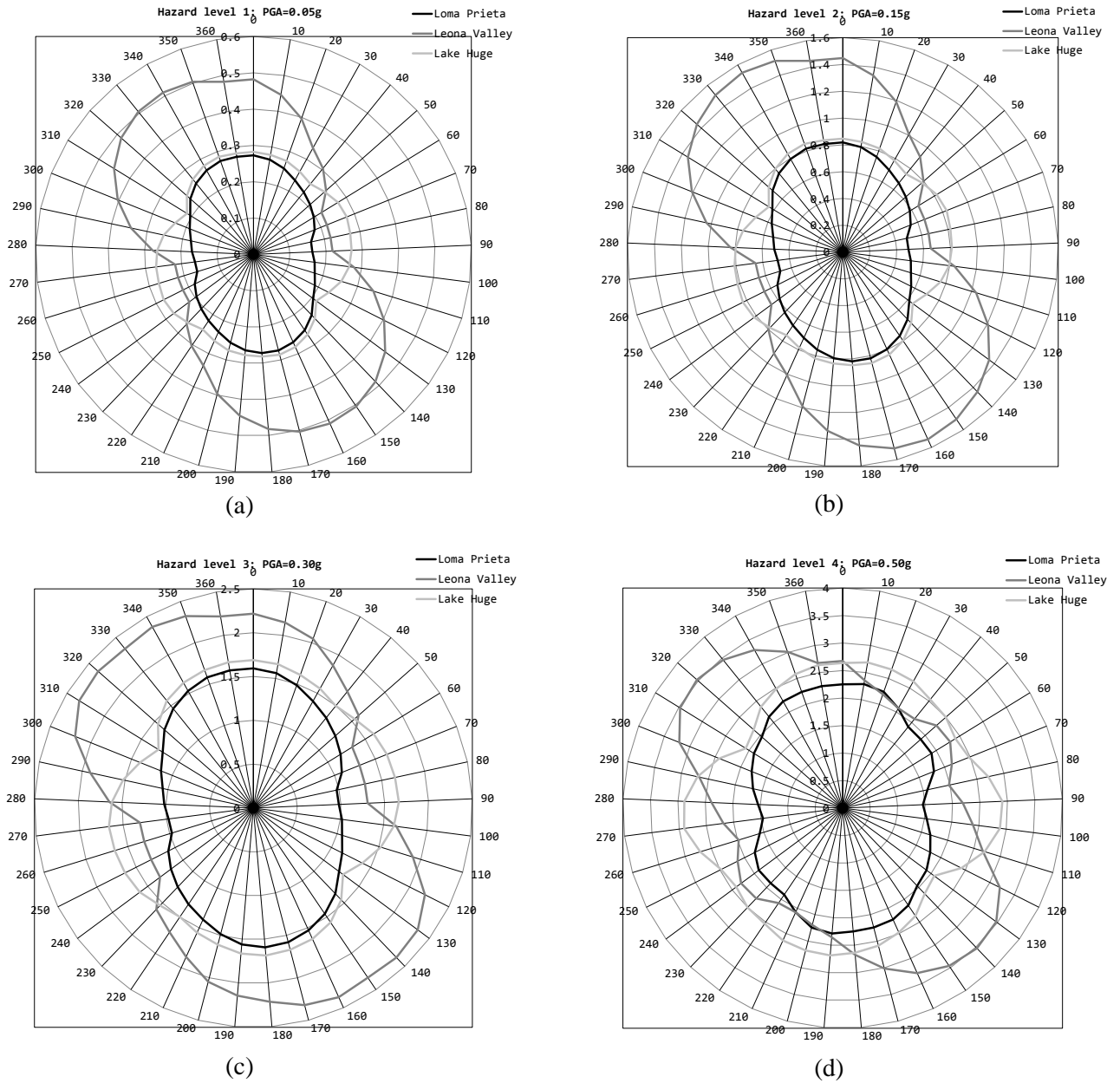


Figure 5. Two-storey steel test example-maximum interstorey drift profiles (a) 50/50, (b) 10/50 and (c) 2/50 hazard levels

Downloaded from ijoce.iust.ac.ir at 8:01 IRDT on Monday May 28th 2018

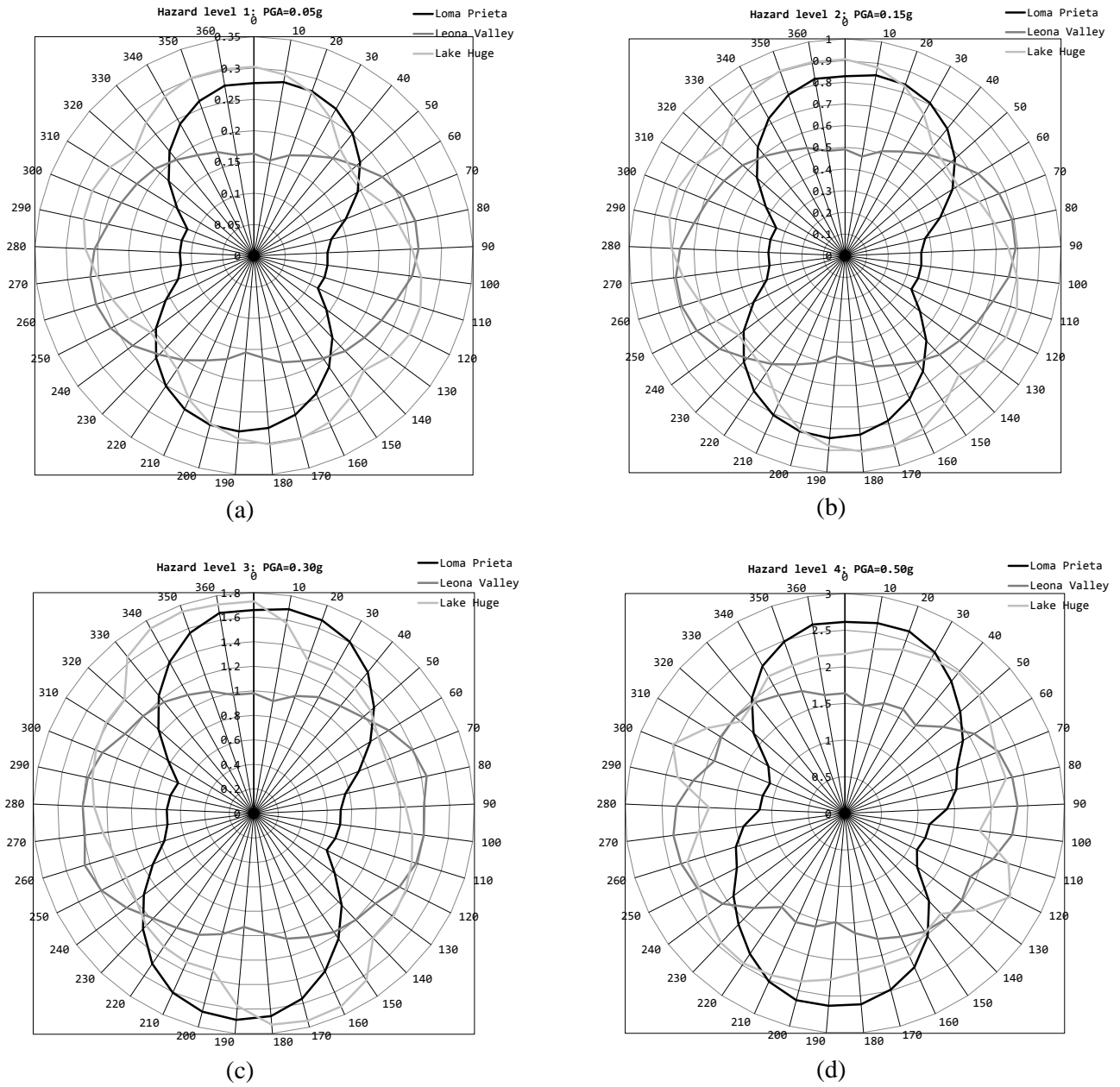


Figure 6. Four-storey steel test example- maximum interstorey drift profiles (a) 50/50, (b) 10/50 and (b) 2/50 hazard levels

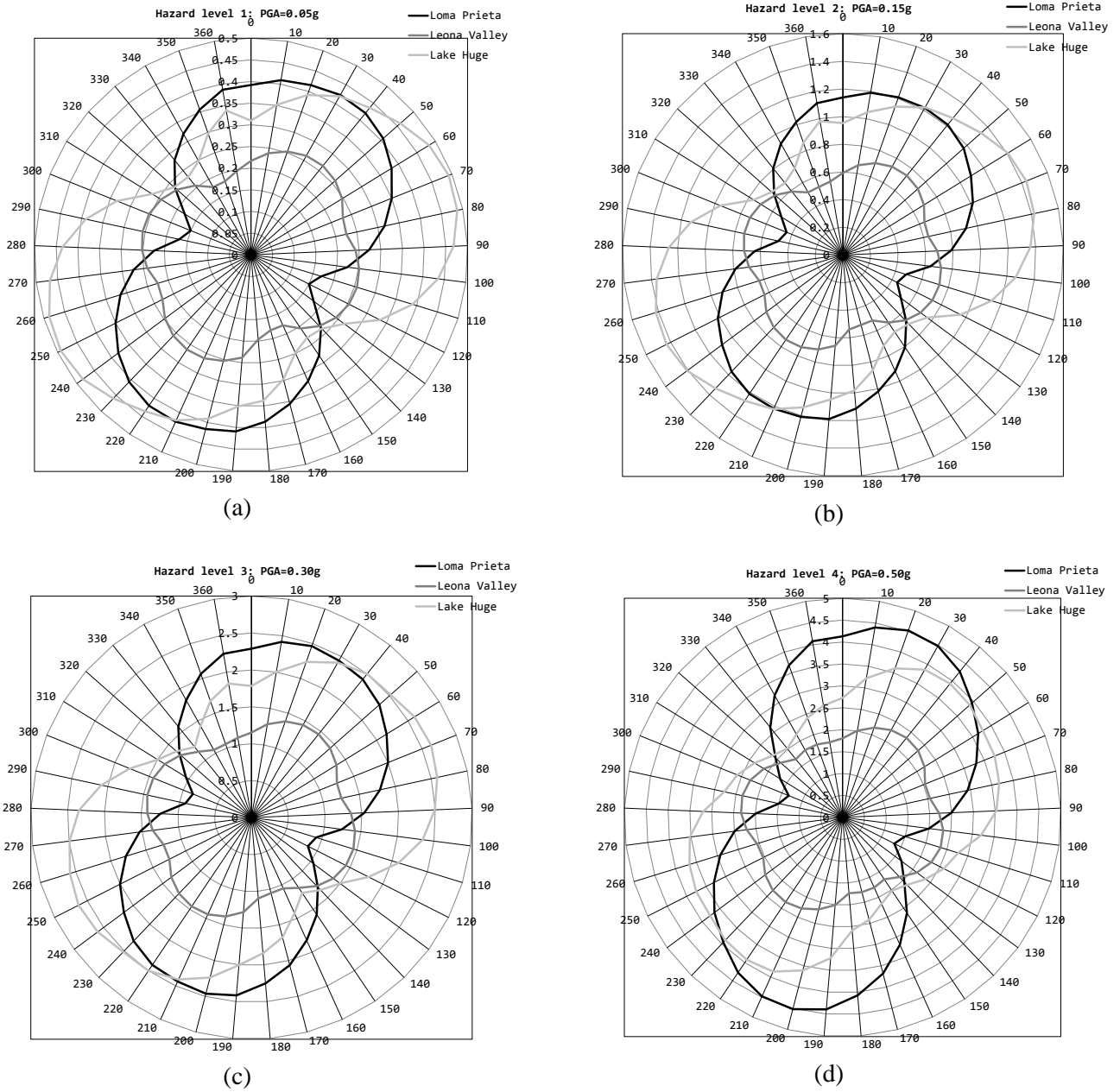


Figure 7. Eight-storey steel test example- maximum interstorey drift profiles (a) 50/50, (b) 10/50 and (b) 2/50 hazard levels



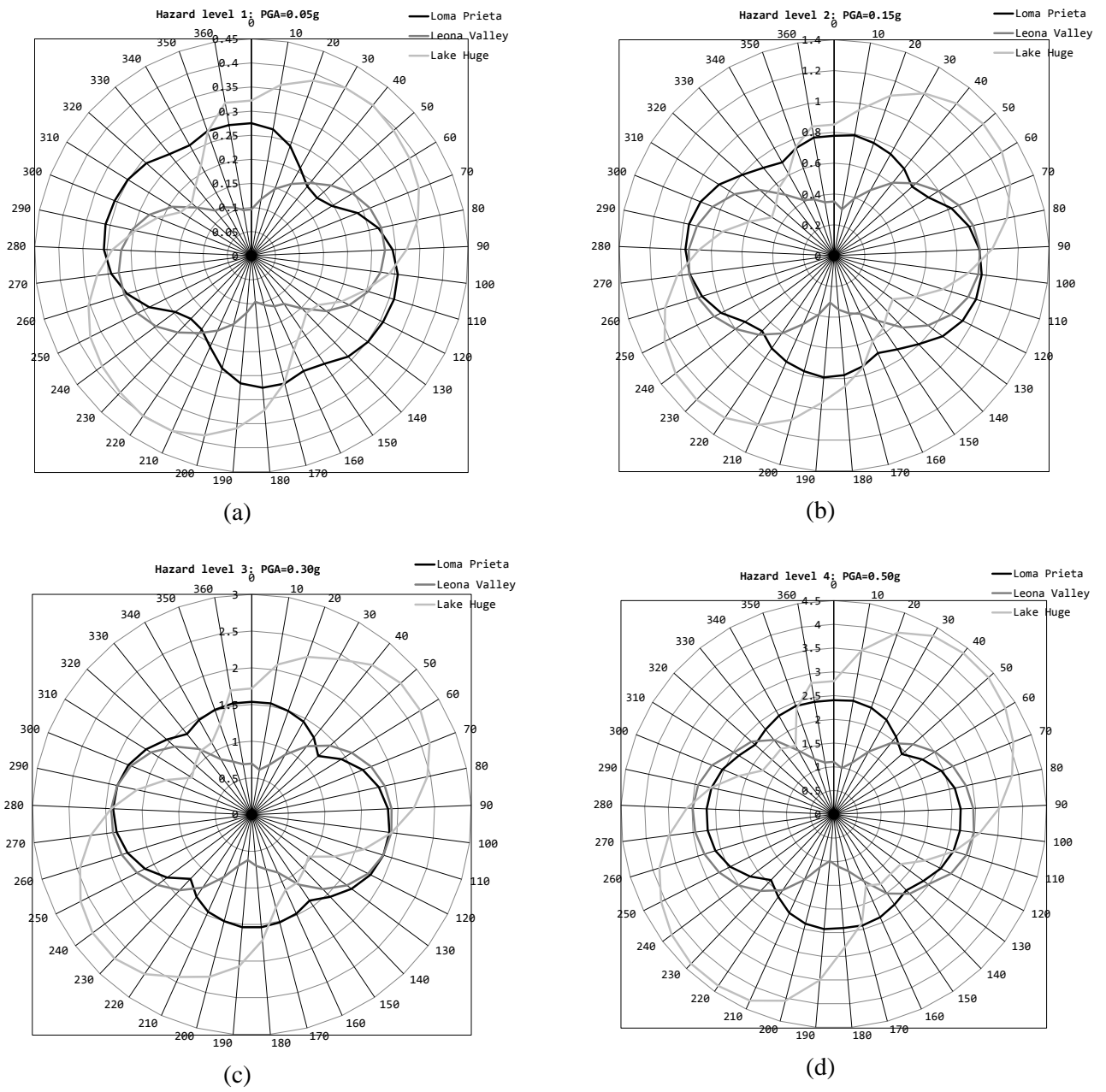


Figure 8. Two-storey steel-RC composite test example-maximum interstorey drift profiles (a) 50/50, (b) 10/50 and (b) 2/50 hazard levels

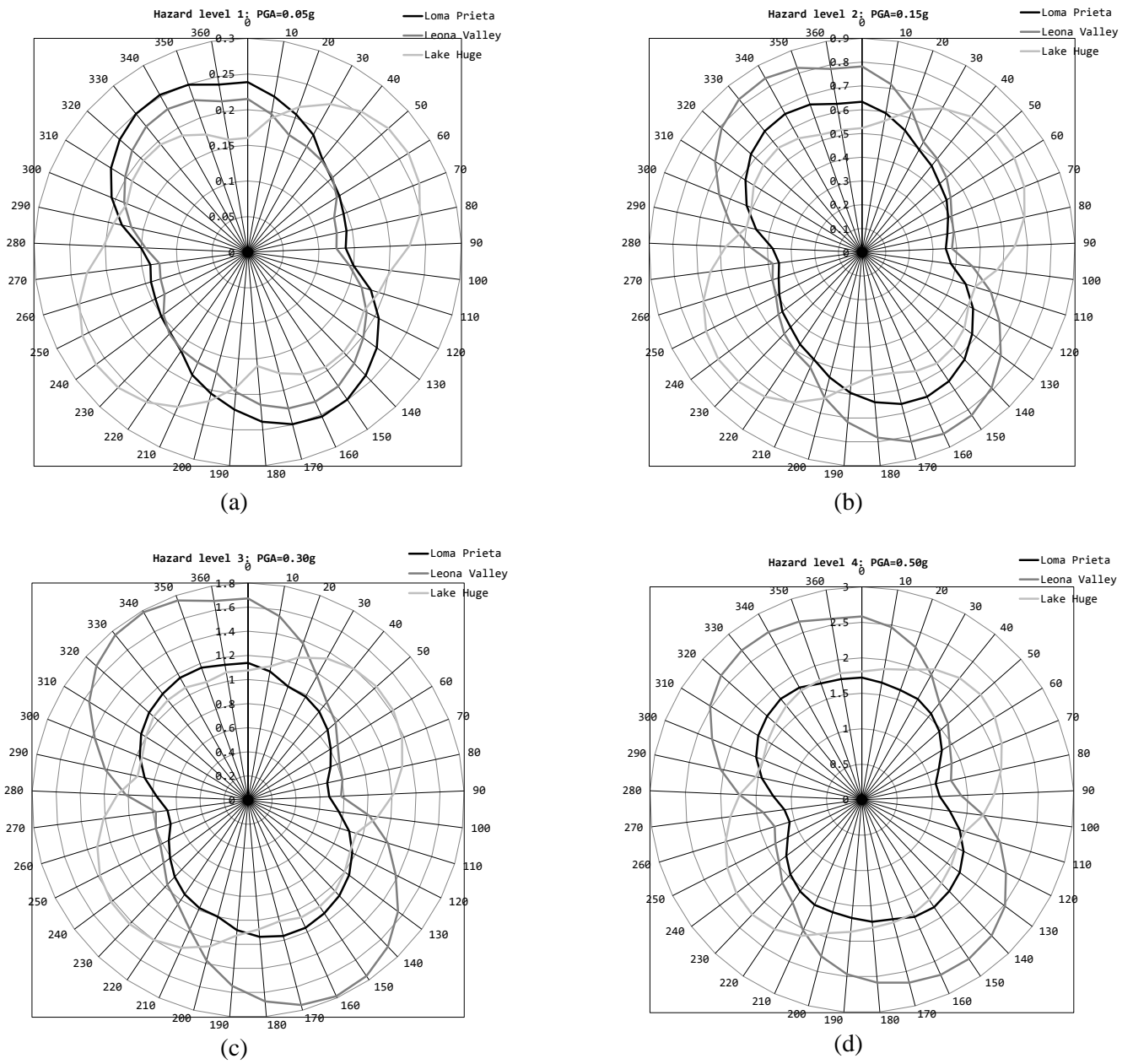


Figure 9. Four-storey steel-RC composite test example- maximum interstorey drift profiles (a) 50/50, (b) 10/50 and (b) 2/50 hazard levels

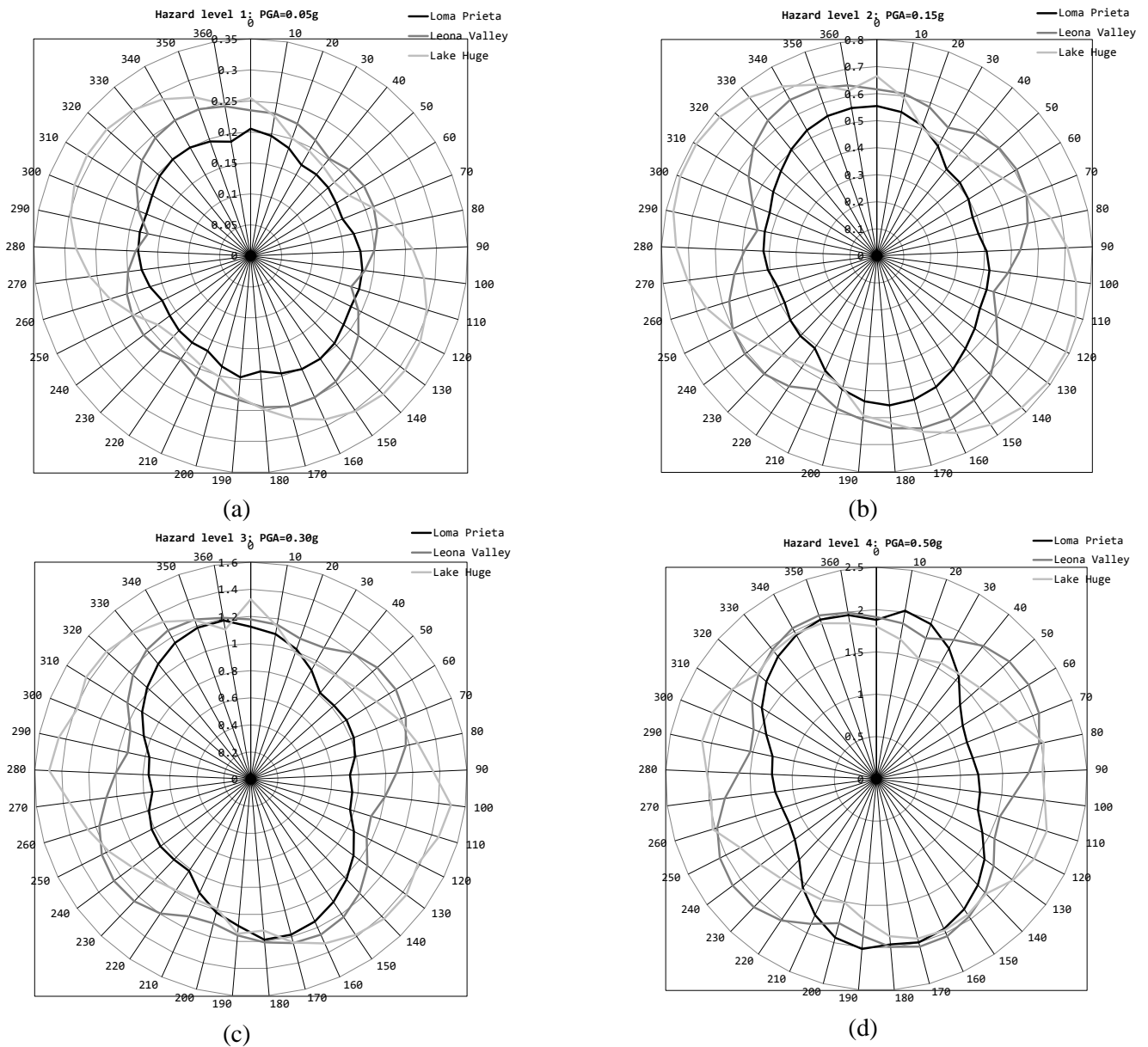


Figure 10. Eight-storey steel-RC composite test example- maximum interstorey drift profiles (a) 50/50, (b) 10/50 and (b) 2/50 hazard levels

8.2 Formulation of the optimization problem

In the second part the structures have been designed based on a PBD optimization framework where the MIDA analysis is implemented. The structural elements (columns, beams and bracings) are separated into groups as shown in Fig. 4(a). Four groups are defined for the columns one for the beams and one for the bracings. The columns are chosen from a database of 24 HEB sections, the beams are chosen from a database of 18 IPE sections while the bracings are chosen from a database of 50 L sections with equal legs. For

the case of the steel-RC composite buildings the columns are encased in concrete quadratic section  $b \times b$  cm<sup>2</sup>, where  $b$  is an additional design variable also defined through the optimization procedure.

The problem formulations are defined based on expression given in Eq. (2), while the drift limits required in the performance-based constraint functions ( $g^{PB}$ ) are provided in Tables 2 and 3, for the steel and steel-RC buildings respectively. More specifically, three performance objectives have been considered corresponding to the (II) Slight, (IV) Moderate and (VII) Collapsed limit states (as defined in Tables 2 and 3) combined with the three hazard levels, i.e. the 50/50, 10/50 and 2/50 hazard levels.

Table 2: Limit state drift ratio limits for the steel moment resisting frames [33]

Limit State	$\theta$ (%) Steel		
	Two-storey	Four-storey	Eight-storey
(I) - None	$\theta \leq 0.30$	$\theta \leq 0.20$	$\theta \leq 0.15$
(II) - Slight	$0.30 < \theta \leq 0.36$	$0.20 < \theta \leq 0.23$	$0.15 < \theta \leq 0.18$
(III) - Light	$0.36 < \theta \leq 0.56$	$0.23 < \theta \leq 0.37$	$0.18 < \theta \leq 0.28$
(IV) - Moderate	$0.56 < \theta \leq 1.20$	$0.27 < \theta \leq 0.80$	$0.28 < \theta \leq 0.60$
(V) - Heavy	$1.20 < \theta \leq 3.00$	$0.80 < \theta \leq 2.00$	$0.60 < \theta \leq 1.50$
(VI) - Major	$3.00 < \theta \leq 8.00$	$2.00 < \theta \leq 5.33$	$1.50 < \theta \leq 4.00$
(VII) - Collapsed	$\theta > 8.00$	$\theta > 5.33$	$\theta > 4.00$

Table 3: Limit state drift ratio limits for the steel-RC composite moment resisting frames [33]

Limit State	$\theta$ (%) Composite		
	Two-storey	Four-storey	Eight-storey
(I) - None	$\theta \leq 0.10$	$\theta \leq 0.07$	$\theta \leq 0.05$
(II) - Slight	$0.10 < \theta \leq 0.20$	$0.07 < \theta \leq 0.13$	$0.05 < \theta \leq 0.10$
(III) - Light	$0.20 < \theta \leq 0.40$	$0.13 < \theta \leq 0.27$	$0.10 < \theta \leq 0.20$
(IV) - Moderate	$0.40 < \theta \leq 1.20$	$0.27 < \theta \leq 0.80$	$0.20 < \theta \leq 0.60$
(V) - Heavy	$1.20 < \theta \leq 3.00$	$0.80 < \theta \leq 2.00$	$0.60 < \theta \leq 1.50$
(VI) - Major	$3.00 < \theta \leq 8.00$	$2.00 < \theta \leq 5.33$	$1.50 < \theta \leq 4.00$
(VII) - Collapsed	$\theta > 8.00$	$\theta > 5.33$	$\theta > 4.00$

For the purposes of the present investigation the two storey test examples are considered and six cases (three designs for each type of building) were examined, implementing different design characteristics into the formulation of the optimization problem. In particular STD1, STD2 and STD3 stand for the two storey steel designs with bracings (4 design variables for the columns, 1 for the beams and 1 for the bracings, 6 in total). COD1, COD2 and COD3 stand for the two storey steel-RC composite designs with bracings (8 design variables for the columns, 1 for the beams and 1 for the bracings, 10 in total). STD1 and COD1 are the optimum designs obtained through the solution of six different formulations where the incident angle is 0°, 30°, 60°, 90°, 120° and 150°, STD2 and COD2 are the optimum designs based on the formulation with the Eurocode constraints checks while STD3 and COD3 are the optimum designs for the critical incident angles obtained from the sensitivity analysis given in Figs. 5 and 8 respectively.

## 9. CONCLUDING REMARKS

In the this work, structural optimization problems are formulated for steel and steel-reinforced concrete composite building structures in order to assess the designs obtained and in particular the efficiency of different design practices, i.e. steel or composite. For the needs of this study, 3D steel and steel-reinforced concrete composite buildings with regular plan views have been considered. In general optimum designs obtained for different incident angles and according to the Eurocodes are examined. In general it can be said that designs with composite encased columns and steel beams correspond to improved performance compared to the steel framed design, while the initial cost is almost the same for all cases considered.

**Acknowledgement:** This research has been financed by the State Scholarships Foundation-IKY for supporting Post-doctoral studies - Research Funding Program: “Multicriteria Design of RC Structures based on Economy, Strength and Energy-Ecological Efficiency”.

## REFERENCES

1. ASCE/SEI Standard 41-06. Seismic Rehabilitation of Existing Buildings, prepublication edition, Structural Engineering Institute, American Society of Civil Engineers, 2006.
2. FEMA-445: *Next-generation Performance-based Seismic Design Guidelines, Program Plan for New and Existing Buildings*, Federal Emergency Management Agency, Washington, DC, 2006.
3. ATC-58, *Guidelines for Seismic Performance Assessment of Buildings*, Applied Technology Council, Redwood City, 2009.
4. Fajfar P. A nonlinear analysis method for performance-based seismic design, *Earthq Spectra* 2000; **16**(3): 573-92.
5. Chopra AK, Goel RK. A modal pushover analysis procedure for estimating seismic demands for buildings, *Earthq Eng Struct Dynam* 2002; **31**(3): 561-82.
6. Vamvatsikos D, Cornell CA. Incremental dynamic analysis, *Earthq Eng Struct Dynam* 2002; **31**(3): 491-514.
7. Lagaros ND. Multicomponent incremental dynamic analysis considering variable incident angle, *Struct Infrastruct Eng* 2010; **6**(1-2): 77-94.
8. Lagaros ND. The impact of the earthquake incident angle on the seismic loss estimation, *Eng Struct* 2010; **32**: 1577-89.
9. Fuyama H, Krawinkler H, Law KH. Drift control in moment resisting steel frame structures, *Struct Des Tall Build* 1994; **3**(3): 163-81.
10. Beck JL, Chan E, Irfanoglu A, Papadimitriou C. Multi-criteria optimal structural design under uncertainty, *Earthq Eng Struct Dynam* 1999; **28**(7): 741-61.
11. Ganzerli S, Pantelides CP, Reaveley LD. Performance-based design using structural optimization, *Earthq Eng Struct Dynam* 2000; **29**(11): 1677-90.

12. Esteva L, Díaz-López O, García-Pérez J, Sierra G, Ismael E. Life-cycle optimization in the establishment of performance-acceptance parameters for seismic design, *Struct Safety* 2002; **24**(2-4): 187-204.
13. Khajepour S, Grierson DE. Profitability versus safety of high rise office buildings, *Struct Multidiscip Optim* 2003; **25**(4): 279-93.
14. Li G, Cheng G. Damage-reduction-based structural optimum design for seismic RC frames, *Struct Multidiscip Optim* 2003; **25**(4): 294-306.
15. Chan C-M, Zou X-K. Elastic and inelastic drift performance optimization for reinforced concrete buildings under earthquake loads, *Earthq Eng Struct Dynam* 2004; **33**(8): 929-50.
16. Liu M, Burns SA, Wen YK. Multiobjective optimization for performance-based seismic design of steel moment frame structures, *Earthq Eng Struct Dynam* 2005; **34**(3): 289-306.
17. Chan C-M, Wang Q. Optimal drift design of tall reinforced concrete buildings with non-linear cracking effects, *Struct Des Tall Special Build* 2005; **14**(4): 331-51.
18. Fragiadakis M, Lagaros ND, Papadrakakis M. Performance based earthquake engineering using structural optimization tools, *Int J Reliability Safety* 2006; **1**(1/2): 59-76.
19. FEMA-350: Recommended Seismic Design Criteria for New Steel Moment-Frame Buildings. Federal Emergency Management Agency, Washington DC, 2000.
20. Fragiadakis M, Lagaros ND, Papadrakakis M. Performance-based multiobjective optimum design of steel structures considering life-cycle cost, *Struct Multidiscip Optim* 2006; **32**(1): 1-11.
21. Foley CM, Pezeshk S, Alimoradi A. Probabilistic performance-based optimal design of steel moment-resisting frames. I: Formulation, *J Struct Eng* 2007; **133**(6): 757-66.
22. Lagaros ND, Papadrakakis M. Seismic design of RC structures: a critical assessment in the framework of multi-objective optimization, *Earthq Eng Struct Dynam* 2007; **36**(12): 1623-39.
23. Rojas HA, Pezeshk S, Foley CM. Performance-based optimization considering both structural and nonstructural components, *Earthq Spectra* 2007; **23**(3): 685-709.
24. Fragiadakis M, Papadrakakis M. Performance-based optimum seismic design of reinforced concrete structures, *Earthq Eng Struct Dynam* 2008; **37**(6): 825-44.
25. Mitropoulou ChCh, Lagaros ND, Papadrakakis M. Building design based on energy dissipation: a critical assessment, *Bulletin Earthq Eng* 2010; **8**(6): 1375-96.
26. Lagaros ND, Naziris IA, Papadrakakis M. The influence of masonry infill walls in the framework of the performance-based design, *J Earthq Eng* 2010; **14**(1): 57-79.
27. Kaveh A, Farahmand Azar B, Hadidi A, Rezazadeh Sorochi F, Talatahari S. Performance-based seismic design of steel frames using ant colony optimization, *J Construct Steel Res* 2010; **66**(4): 566-74.
28. Lagaros ND, Fragiadakis M. Evaluation of ASCE-41, ATC-40 and N2 static pushover methods based on optimally designed buildings, *Soil Dynam Earthq Eng* 2011; **31**(1): 77-90.
29. Esteva L, Campos D, Díaz-López O. Life-cycle optimisation in earthquake engineering, *Struct Infrastruct Eng* 2011; **7**(1): 33-49.
30. Al-Ansari M, Senouci A. Drift optimization of high-rise buildings in earthquake zones, *Struct Des Tall Special Build* 2011; **20**(2): 208-22.

31. Fragiadakis M, Lagaros ND. An overview to structural seismic design optimisation frameworks, *Comput Struct* 2011; **89**(11-12): 1155-65.
32. Mitropoulou ChCh, Lagaros ND, Papadrakakis M. Life-cycle cost assessment of optimally designed reinforced concrete buildings under seismic actions, *Reliability Eng Syst Safety* 2011; **96**: 1311-31.
33. Lagaros ND, Magoula E. Life-cycle cost assessment of mid-rise and high-rise steel and steel-reinforced concrete composite minimum cost building designs, *Struct Des Tall Special Build* 2013; **22**(12): 954-74.
34. Kaveh A, Bakhshpoori T, Azimi M. Seismic optimal design of 3D steel frames using cuckoo search algorithm, *Struct Des Tall Special Build* 2015; **24**(3): 210-27.
35. Penzien J, Watabe M. Characteristics of 3-dimensional earthquake ground motions, *Earthq Eng Struct Dynam* 1975; **3**(4): 365-73.
36. Wilson EL, Suharwardy A, Habibullah A. A clarification of the orthogonal effects in a tree-dimensional seismic analysis, *Earthq Spectra* 1995; **11**(4): 659-66.
37. Lopez OA, Torres R. The critical angle of seismic incidence and the maximum structural response, *Earthq Eng Struct Dynam* 1997; **26**: 881-94.
38. Menun C, Der Kiureghian A. A replacement for the 30%, 40% and SRSS rules for multicomponent seismic analysis, *Earthq Spectra* 1998; **14**(1): 153-63.
39. Lopez OA, Chopra AK, Hernandez JJ. Critical response of structures to multicomponent earthquake excitation, *Earthq Eng Struct Dynam* 2000; **29**: 1759-78.
40. Lopez OA, Chopra AK, Hernandez JJ. Evaluation of combination rules for maximum response calculation in multicomponent seismic analysis, *Earthq Eng Struct Dynam* 2001; **30**: 1379-98.
41. Menun C, Der Kiureghian A. Envelopes for seismic response vectors. I: theory, *J Struct Eng* 2000; **126**: 467-73.
42. Menun C, Der Kiureghian A. Envelopes for seismic response vectors. II: application, *J Struct Eng* 2000; **126**: 474-81.
43. Anastassiadis K, Avramidis I, Panetsos P. Concurrent design forces in structures under three-component orthotropic seismic excitation, *Earthq Spectra* 2002; **18**: 1-17.
44. MacRae GA, Mattheis J. Three-dimensional steel building response to near-fault motions, *J Struct Eng* 2000; **126**(1): 117-26.
45. MacRae GA, Tagawa H. Seismic behaviour of 3D steel moment frame with biaxial columns, *J Struct Eng* 2001; **127**(5): 490-7.
46. Gherzi A, Rossi PP. Influence of bi-directional ground motions on the inelastic response of one-storey in-plan irregular systems, *Eng Struct* 2001; **23**(6): 579-91.
47. Athanatopoulou AM. Critical orientation of three correlated seismic components, *Eng Struct* 2005; **27**(2): 301-12.
48. Rigato AB, Medina RA. Influence of angle of incidence on seismic demands for inelastic single-storey structures subjected to bi-directional ground motions, *Eng Struct* 2007; **29**(10): 2593-2601.
49. Krawinkler H, Miranda E. Performance-based earthquake engineering, In: *Earthquake Engineering: From Engineering Seismology to Performance-based Earthquake Engineering* (Y. Bozorgnia and Vitelmo V. Bertero (Eds), CRC Press, 2004.

50. EC3. Eurocode 3: Design of steel structures - Part 1-1: General rules and rules for buildings, ENV 1993-1-1:1992, CEN European Committee for standardization, Brussels, 2005.
51. McKenna F, Fenves GL. The OpenSees Command Language Manual - Version 1.2. Pacific Earthquake Engineering Research Centre, University of California, Berkeley, 2001.
52. Kent DC, Park R. Flexural members with confined concrete, *J Struct Div* 1971; **97**(7): 1969-90.
53. Tremblay R. Inelastic seismic response of steel bracing members, *J Construct Steel Res* 2002; **58**(5-8): 665-701.